# Effects of Feeding *Spodoptera littoralis* on Lima Bean Leaves. III. Membrane Depolarization and Involvement of Hydrogen Peroxide[1]

**Massimo E. Maffei*, Axel Mithöfer, Gen-Ichiro Arimura, Hannes Uchtenhagen, Simone Bossi, Cinzia M. Bertea, Laura Starvaggi Cucuzza, Mara Novero, Veronica Volpe, Stefano Quadro, and Wilhelm Boland**

Department of Plant Biology and Centre of Excellence CEBIOVEM, University of Turin, I–10125 Turin, Italy (M.E.M, S.B., C.M.B., L.S.C., M.N., V.V., S.Q.); and Max Planck Institute for Chemical Ecology, Bioorganic Chemistry, D–07745 Jena, Germany (A.M., G.-I.A., H.U., W.B.)

In response to herbivore (*Spodoptera littoralis*) attack, lima bean (*Phaseolus lunatus*) leaves produced hydrogen peroxide ($H_2O_2$) in concentrations that were higher when compared to mechanically damaged (MD) leaves. Cellular and subcellular localization analyses revealed that $H_2O_2$ was mainly localized in MD and herbivore-wounded (HW) zones and spread throughout the veins and tissues. Preferentially, $H_2O_2$ was found in cell walls of spongy and mesophyll cells facing intercellular spaces, even though confocal laser scanning microscopy analyses also revealed the presence of $H_2O_2$ in mitochondria/peroxisomes. Increased gene and enzyme activations of superoxide dismutase after HW were in agreement with confocal laser scanning microscopy data. After MD, additional application of $H_2O_2$ prompted a transient transmembrane potential ($V_m$) depolarization, with a $V_m$ depolarization rate that was higher when compared to HW leaves. In transgenic soybean (*Glycine max*) suspension cells expressing the $Ca^{2+}$-sensing aequorin system, increasing amounts of added $H_2O_2$ correlated with a higher cytosolic calcium ($[Ca^{2+}]_{cyt}$) concentration. In MD and HW leaves, $H_2O_2$ also triggered the increase of $[Ca^{2+}]_{cyt}$, but MD-elicited $[Ca^{2+}]_{cyt}$ increase was more pronounced when compared to HW leaves after addition of exogenous $H_2O_2$. The results clearly indicate that $V_m$ depolarization caused by HW makes the membrane potential more positive and reduces the ability of lima bean leaves to react to signaling molecules.

In response to pathogen invasion, plants mount a broad range of defense responses, including the generation of reactive oxygen species (ROS; Lamb and Dixon, 1997; Mur et al., 2005). ROS are also generated in plant tissues in response to wounding (Angelini et al., 1990; Bradley et al., 1992; Olson and Varner, 1993; Felton et al., 1994; Bi and Felton, 1995; Orozco-Cárdenas and Ryan, 1999), mechanical stimulation of isolated cells (Yahraus et al., 1995; Gus-Mayer et al., 1998), and the treatment of cell suspension cultures with elicitors (Legendre et al., 1993; Mithöfer et al., 1997; Stennis et al., 1998). ROS also have been associated with plant herbivore interactions (Mithöfer et al., 2004; Leitner et al., 2005), and oxidative changes in the plants correspond with oxidative damage in the midguts of insects feeding on previously wounded plants (Orozco-Cárdenas and Ryan, 1999). In pathogenic interactions, wound-induced ROS accumulation, in particular hydrogen peroxide ($H_2O_2$), is observed both locally and systemically in leaves of several plant species (Mehdy et al., 1996; Bergey et al., 1999; Orozco-Cárdenas and Ryan, 1999; Orozco-Cárdenas et al., 2001). In some cases, especially under stress conditions, a rapid and transient production of high levels of ROS may reach intracellular concentrations of up to 1 M $H_2O_2$ in about 13 min (Jacks and Davidonis, 1996). In response to herbivores, $H_2O_2$ levels are likely to be elevated as long as the attacks persist. Bi and Felton (1995) have proposed that herbivore attacks can cause a localized oxidative response in soybean (*Glycine max*) leaves and have identified some potential functions of ROS that might affect plant-herbivore interactions. Furthermore, the presence of $H_2O_2$ in the plant in response to herbivory, before any subsequent secondary pathogen invasion, could be advantageous because timing of the induction of defense responses can be an important factor in the success or failure of plants to defend against pathogen attacks (Dangl et al., 1996), and wound-generated $H_2O_2$ that occurs in the veins also could have a defensive role against bacteria, fungi, or viruses, as they may invade leaves wounded by herbivores (Orozco-Cárdenas and Ryan, 1999). ROS also represent second messengers that eventually activate downstream defense reactions (Foyer and Noctor, 2005), such as synthesis of pathogenesis-related proteins (Chen et al., 1993), glutathione *S*-transferase, glutathione

[1] This work was supported by the Fonds der Chemischen Industrie (Frankfurt a.M.) from the Centre of Excellence for Plant and Microbial Biosensing (Turin) and local research grants from the University of Turin, Italy.

* Corresponding author; e-mail massimo.maffei@unito.it; fax 390–112365967.

The author responsible for distribution of materials integral to the findings presented in this article in accordance with the policy described in the Instructions for Authors (www.plantphysiol.org) is: Massimo E. Maffei (massimo.maffei@unito.it).

Article, publication date, and citation information can be found at www.plantphysiol.org/cgi/doi/10.1104/pp.105.071993.

peroxidase (GPX), and ubiquitin (Levine et al., 1994), as well as phytoalexin accumulation (Devlin and Gustine, 1992; Mithöfer et al., 2004) and production of herbivore-induced volatile products (Mithöfer et al., 2004).

The induction of the oxidative burst is often dependent on $Ca^{2+}$, which has been demonstrated several times (e.g. Price et al., 1994; Low and Merida, 1996; Cazalé et al., 1998). Electrophysiological studies revealed the existence of plasma membrane $Ca^{2+}$-permeable channels activated by membrane depolarization or hyperpolarization in response to environmental stimuli (for review, see White, 2000; Sanders et al., 2002) and at the very edge of herbivore wounding in plant-insect interactions (Maffei et al., 2004). ROS can interact with ion channel activity, and oxidase-dependent electron transfer could drive a transmembrane potential ($V_m$) depolarization; both effects lead to channel activation. This regulation of ion channels by $H_2O_2$ in plants has been indicated (Cazalé et al., 1998; Pei et al., 2000; Foreman et al., 2003; Overmyer et al., 2003) but has never been analyzed in plant herbivore interaction, to our knowledge. Thus, the aim of this study was to analyze the role of $H_2O_2$ in plant-herbivore interactions.

By taking advantage of the model system consisting of *Spodoptera littoralis* larvae feeding on lima bean (*Phaseolus lunatus*) leaves (Maffei et al., 2004; Mithöfer et al., 2005), we used several microscopic, physiological, biochemical, and molecular biological tools to evaluate the role of $H_2O_2$ in plant-herbivore interactions. Thus, we investigated (1) the cellular and subcellular $H_2O_2$ localization in mechanically damaged (MD) and *S. littoralis* herbivore-wounded (HW) tissues by means of fluorescence light microscopy, confocal laser-scanning microscopy (CLSM), and transmission electron microscopy; (2) the effect of $H_2O_2$ on $[Ca^{2+}]_{cyt}$ using CLSM and apoaequorin-transformed plants; (3) the effect of $H_2O_2$ on $V_m$ and cytosolic calcium ($[Ca^{2+}]_{cyt}$) variations using specific ion channel inhibitors in MD and HW tissues; and (4) the enzyme activity and quantitative gene expression of some ROS scavenging systems. We show that $H_2O_2$ is released upon HW and MD in plant tissues. We also demonstrate that $H_2O_2$ release caused $V_m$ depolarization involving $Ca^{2+}$ channels. Furthermore, we show that the HW-induced $V_m$ depolarization is a crucial event that, by depolarizing the membrane potential, reduces the ability of lima bean leaves to react to signaling molecules. Finally, we show that increased $H_2O_2$ accumulation in HW leaves is correlated to increased superoxide dismutase (SOD) enzyme activity and gene expression.

## RESULTS

### Cellular and Subcellular Localization of $H_2O_2$ in MD and HW Lima Bean Tissues

ROS play two divergent roles in plant adaptation to the changing environment: enhancement of damage by a highly oxidizing microenvironment or mediating the activation of other defense responses under certain biotic and abiotic stresses (Lamb and Dixon, 1997; Yang and Poovaiah, 2002). In contrast to most animal cells, plant cells are able to produce ROS, mainly $H_2O_2$, constitutively in significant amounts, and this production is developmentally regulated by light, phytohormones, or wounding and predominantly associated with the cell's exocellular matrix (ECM; Bolwell and Wojtaszek, 1997; Bolwell, 1999). Mechanical damage of lima bean leaves triggered the production of $H_2O_2$ as can be seen after incubation of tissues with the dye 3,3-diaminobenzidine (DAB; Thordal-Christensen et al., 1997; Orozco-Cárdenas and Ryan, 1999). DAB staining increased in time by spreading throughout the veins and tissues and was mainly localized in the damaged zone (Fig. 1, C and E). The accumulation of $H_2O_2$ occurred near wound sites and also in distal unwounded leaves, indicating that the process might be regulated by a systemic signaling system. When *S. littoralis* was allowed to feed on DAB-incubated leaves, the same reaction was observed and increased with time, with a slightly increased staining with respect to MD leaves (Fig. 1, D and F). Figure 1 also shows the edge of a leaf after 6 h of MD (Fig. 1A) and HW (Fig. 1B) immediately cut before mounting the slides; here, it is clearly visible that in both cases the slicing of leaves causes an immediate $H_2O_2$ release. DAB $H_2O_2$ assay is based on endogenous peroxidases, the levels of which are assumed to be constant. As this is not always the case (as shown, for instance, by Hiraga et al., 2000), direct

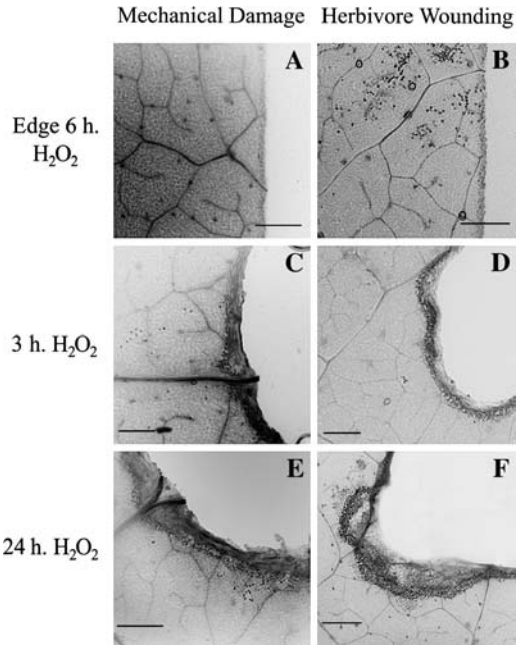


**Figure 1.** Histochemical localization of $H_2O_2$ in MD and HW lima bean leaves after incubation of tissues with the dye DAB. As a control, the first top pictures show the edge of leaf samples of 6 h after MD and HW immediately cut before mounting the slides; it is clearly visible that the preparation of samples causes an immediate $H_2O_2$ release, but the staining is lower if compared to MD and HW tissues after a longer exposure. Metric bar = 1 mm.

measurements using cerium chloride have been used as a more accurate approach (Bestwick et al., 1998; Mur et al., 2000). Figure 2 shows subcellular localization of $H_2O_2$ in HW (Fig. 2, A–C) and MD (Fig. 2, D–F) lima bean leaves as a function of the distance from the wound zone. In general, the appearance of $CeCl_3$ deposits of variable intensity occurred in the cell walls of spongy and mesophyll cells facing intercellular spaces. A strong and evident $CeCl_3$ precipitation was visible in both HW and MD tissues at the very edge of wound (Fig. 2, A and D). At about 500 $\mu$m from the bite (Fig. 2B) or MD (Fig. 2E) zone, accumulation of $H_2O_2$ was still at high levels; however, at longer distances staining fades in MD tissues (Fig. 2F), whereas it remained high in HW tissues (Fig. 2C).

To better evaluate the difference between $H_2O_2$ production in HW and MD, CLSM was performed using 2′,7′-dichlorofluorescin diacetate ($H_2$DCF-DA; Lee et al., 1999; Pei et al., 2000; Fig. 3). No significant

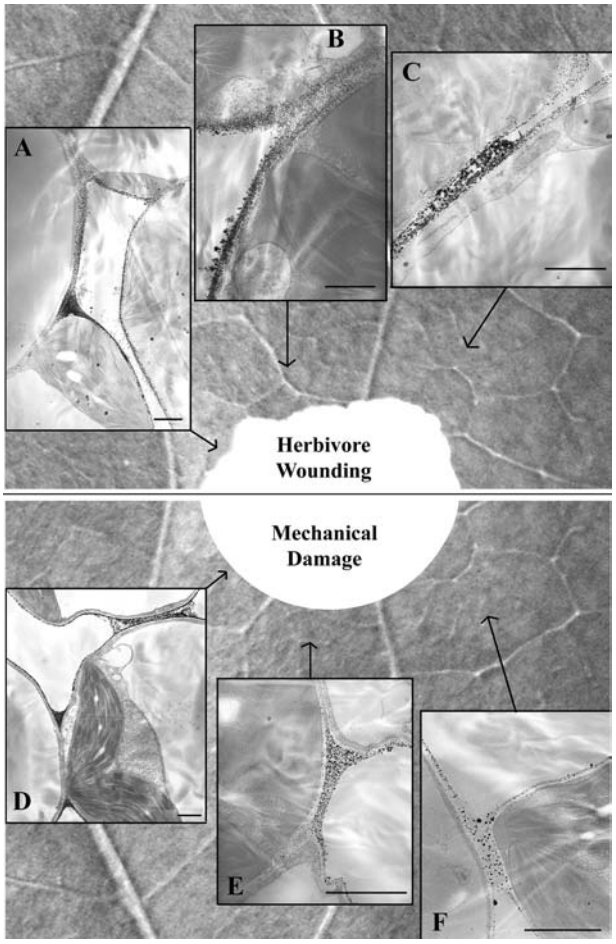


**Figure 2.** Subcellular $H_2O_2$ localization in HW and MD lima bean leaves. A to C, HW leaves. A, Very close to the bite zone, a strong cerium chloride precipitation is visible. B, At 500 to 600 $\mu$m from the bite zone. C, At 3 mm from the bite zone. D to F, MD leaves. D, Very close to the wound zone, a strong cerium chloride precipitation is visible. E, At 500 to 600 $\mu$m from the wound zone. F, At 3 mm from the wound zone. Metric bar = 1 $\mu$m.

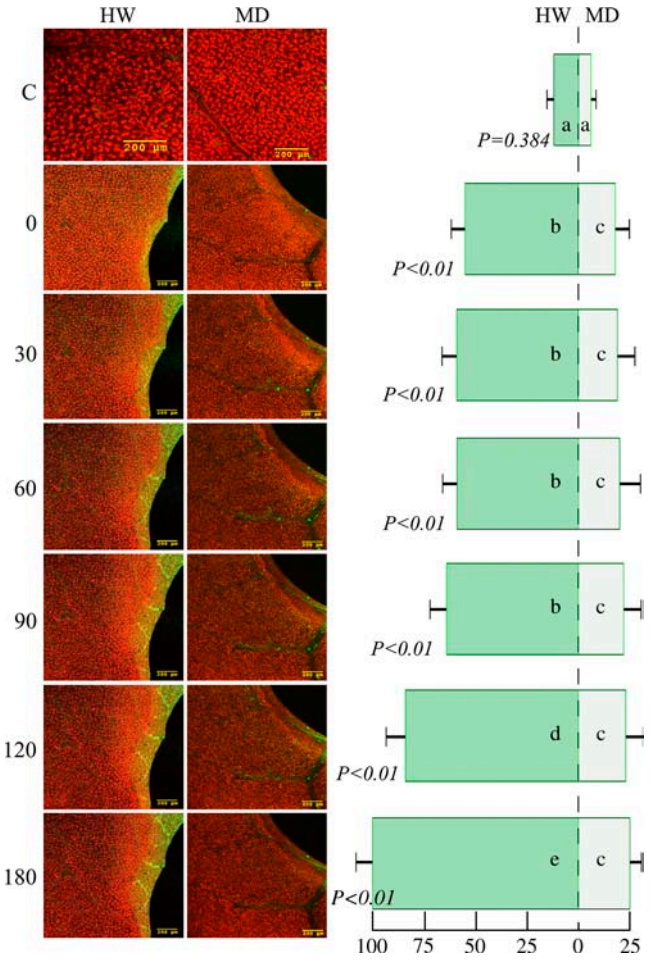


**Figure 3.** False-color image analysis reconstructions from confocal laser-scanning microscope observations and fluochemical localization of $H_2O_2$ in an image analysis. The production of $H_2O_2$ by HW and MD lima bean leaves was examined by loading leaves with $H_2$DCF-DA. This nonfluorescent dye can cross the plasma membrane freely and is then cleaved to its impermeable counterpart, $H_2$DCF, by endogenous esterases. $H_2$DCF, which accumulates in the cell, functions as a reporter of cytoplasmic $H_2O_2$ by converting upon oxidation to its fluorescent form, DCF (green fluorescence). The chloroplasts are evidenced by a bright red color caused by chlorophyll fluorescence. No significant difference was found in control (C) tissues, whereas the image analysis of large portions of HW and MD tissues revealed an increasing $H_2O_2$ fluorescent staining with time in HW tissue that was significantly higher that in MD tissues. Metric bars are indicated on the figures; numbers at the left represent minutes after HW or MD. $H_2O_2$ content is expressed as relative percentage, assuming 100% the highest value obtained (i.e. HW at 180 min). The same letter indicates nonsignificant differences.

difference was found in control tissues (C; Fig. 3, HW and MD), whereas image analysis of large portions of HW and MD tissues revealed a time-dependent increase of $H_2O_2$ fluorescent staining in HW tissue that was significantly higher than in MD tissues (Fig. 3). A multiple comparison test showed that there was a significant difference between MD and HW controls and time 0, but no significant differences were found between time 0 and time 180 min in MD leaves and

between time 0 and time 90 min in HW leaves. Significant increases in $H_2O_2$ levels were found in HW only after 120 min (Fig. 3). 10-Acetyl-3,7-dihydroxyphenoxazine (Amplex Red) was used to detect the presence of active peroxidases and the release of $H_2O_2$ from biological samples, with particular reference to mitochondria (Votyakova and Reynolds, 2001). Figure 4 shows the subcellular localization of $H_2O_2$ production in HW leaves following incubation with Amplex Red. Chloroplasts appear as blue organelles while Amplex Red appears as yellow staining. Mitochondria/peroxisomes are stained in yellow and are localized surrounding chloroplasts (single arrow) and adjacent to the plasma membrane (double arrow). The latter is also stained in yellow. The production of $H_2O_2$ appears not only to be limited to the ECM, as shown by $CeCl_3$ staining, but also involves the protoplast.

### Effect of $H_2O_2$ on Cytosolic $Ca^{2+}$ Variations in Aequorin-Expressing Soybean Cells

Since treatment with $H_2O_2$ can stimulate increases in cytosolic $Ca^{2+}$ (Price et al., 1994; Yang and Poovaiah, 2002), for instance by activating calcium channels (Pei et al., 2000), we first investigated the possibility whether $H_2O_2$ could trigger a $Ca^{2+}$ response in transgenic soybean suspension cells expressing the $Ca^{2+}$-sensitive aequorin system (Mithöfer et al., 1999; Mithöfer and Mazars, 2002). The $Ca^{2+}$ response was determined in a concentration-dependent fashion, and the transiently accumulating $[Ca^{2+}]_{cyt}$ appeared to be linearly correlated with the amount of $H_2O_2$ up to 0.1 mM (Fig. 5).

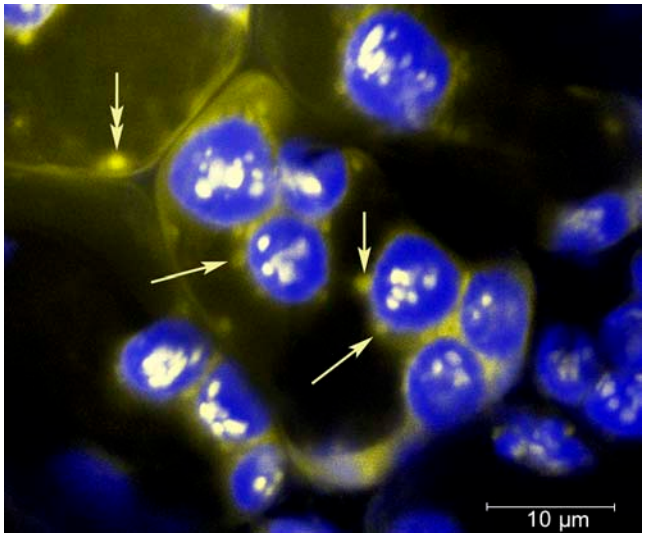


**Figure 4.** False-color CLSM subcellular localization of $H_2O_2$ production in HW lima bean. Chloroplasts are stained in blue; $H_2O_2$ is stained in yellow. Double arrow indicates plasma membrane-associated organelle and single arrows indicate chloroplast-associated organelles, which also appear as bright-yellow spots on chloroplasts. Metric bar is included.

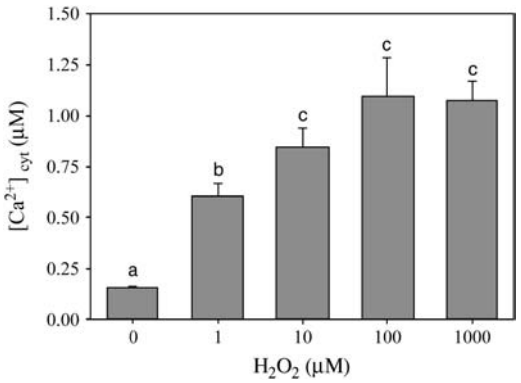


**Figure 5.** Monitoring of $[Ca^{2+}]_{cyt}$ increases in soybean cell suspension cultures expressing the $Ca^{2+}$-sensing aequorin system. Increasing $H_2O_2$ concentrations from 1 up to 100 $\mu$M are positively correlated with increased $[Ca^{2+}]_{cyt}$, which could be detected after 1 min. Above 1,000 $\mu$M no significant variations were observed. Bars indicate SD. Different letters indicate significant differences between treatments ($P < 0.001$) according to univariate ANOVA. Tamhane's T2 test was used to determine post-hoc differences.

At higher concentrations, $[Ca^{2+}]_{cyt}$ did not show statistical differences and remained high.

### Effect of $H_2O_2$ on $V_m$ in MD and HW Lima Bean Tissues

One of the early signals in plant-herbivore interaction is the variation in the $V_m$ (Maffei et al., 2004). Having assessed the dose-response effect of $H_2O_2$ release on $[Ca^{2+}]_{cyt}$, and because of the possible unbalance of charges across the plasma membrane depending on $[Ca^{2+}]_{cyt}$ variations, we analyzed changes in $V_m$ when increasing $H_2O_2$ concentrations (from 0.3 mM to 24 mM) were applied to MD and HW tissues. In MD lima bean, $H_2O_2$ concentrations in the same range used in soybean cell culture experiments triggered $V_m$ depolarization (Fig. 6A), with 18 mM being the highest concentration above which the $V_m$ could not be recovered by washing tissues with a fresh buffer solution. The general trend (except above 18 mM) was a transient strong depolarization that was followed by a constant depolarization for a certain time (Fig. 6A). As reported earlier (Maffei et al., 2004), HW tissues showed a more positive $V_m$ with respect to MD leaves, and the response to $H_2O_2$ was a net lowering of the response (Fig. 6B), even though a direct comparison of MD and HW $V_m$ responses to $H_2O_2$ showed some sort of threshold lowering. Even in HW, $V_m$ was recovered up to 18 mM $H_2O_2$ (Fig. 6B).

The linearization of the data of Figure 6 is given in Table I. The $V_m$ depolarization rate increased linearly in MD leaves from 0.3 to 12 mM $H_2O_2$, whereas in HW leaves linearity was present only up to 3 mM $H_2O_2$. In MD leaves, $H_2O_2$ caused higher depolarizing rates at almost all concentrations when compared to the effect on HW leaves (Table I). These data indicate that the rate of the first $V_m$ depolarization is clearly dependent on starting values of $V_m$ and that $V_m$ depolarization

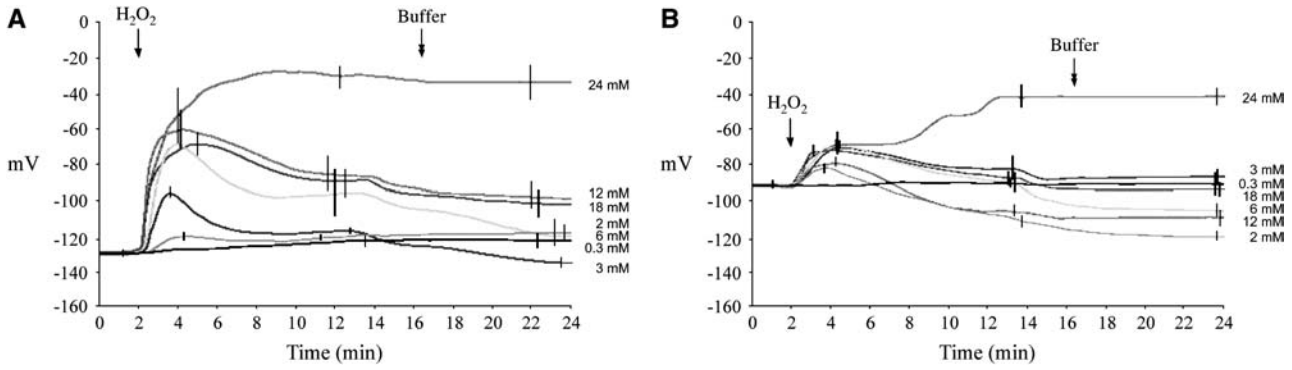


**Figure 6.** Effect of increasing $H_2O_2$ concentrations on $V_m$ of MD (A) and HW (B) lima bean leaves. A, Increasing $H_2O_2$ prompts increased transient $V_m$ depolarization up to 18 mM. Washing tissues with fresh buffer caused $V_m$ hyperpolarization. B, Herbivore-derived wounding caused a significant $V_m$ depolarization (compare starting $V_m$ values in A and B). Increasing $H_2O_2$ concentrations caused a transient $V_m$ depolarization, which is followed by a $V_m$ hyperpolarization. Bars indicate SD.

experienced after HW lowers the plant ability to respond to $H_2O_2$.

### Effect of $H_2O_2$ on $[Ca^{2+}]_{cyt}$ in MD and HW Lima Bean Tissues

Because treatment with $H_2O_2$ stimulated enrichment in $[Ca^{2+}]_{cyt}$, we used the membrane-permeable $Ca^{2+}$-selective fluorescent dye Fluo-3 AM to determine whether $[Ca^{2+}]_{cyt}$ was increased in both MD and HW leaves after the addition of exogenous $H_2O_2$ (Fig. 7). As shown recently (Maffei et al., 2004), HW caused a cellular influx of $Ca^{2+}$ at the very edge of the bite that was significantly different from the one caused by MD (Fig. 7, before $H_2O_2$). Treatment with 15 mM $H_2O_2$ caused an increase in Fluo-3 AM fluorescence in both MD and HW. However, MD leaves showed a stronger $Ca^{2+}$ signal compared to HW (Fig. 7, after $H_2O_2$). No significant increase in $Ca^{2+}$ levels was found in MD between controls and before $H_2O_2$ (Fig. 7).

### Effect of $H_2O_2$ on $[Ca^{2+}]_{cyt}$ and $Ca^{2+}$-Dependent $V_m$ Variations in MD and HW Lima Bean Tissues

Having assessed the direct involvement of $Ca^{2+}$ in response to $H_2O_2$, we studied the effects of some $Ca^{2+}$ channel inhibitors on $V_m$ responses to MD and HW leaves perfused with 15 mM $H_2O_2$.

Since $Ca^{2+}$ can be present and stored in several cell compartments in different forms as well as in the buffering solution, we started by perfusing MD and HW tissues with the $Ca^{2+}$ chelating agent EGTA. Chelation of extracellular $Ca^{2+}$ by EGTA has been found to completely abolish the increase in $[Ca^{2+}]_{cyt}$ and the

**Table I.** *Linearization of $V_m$ variations in MD and HW lima bean leaves*

| $H_2O_2$ Concentration | $V_m$ Depolarization Immediately after $H_2O_2$ Perfusion | | | | |
|---|---|---|---|---|---|
| | MD | | HW | | $P^b$ |
| | Mean | $R^a$ | Mean | $R$ | |
| mM | | | *mV min*$^{-1}$ | | |
| 0.3 | 1.02 | 0.95 | 0.42 | 0.56 | 0.174 |
| 2.0 | 4.83 | 0.97 | 6.67 | 0.99 | 0.061 |
| 3.0 | 25.83 | 0.98 | 10.73 | 0.97 | <0.001 |
| 6.0 | 44.62 | 0.98 | 10.45 | 0.97 | <0.001 |
| 12.0 | 74.12 | 0.95 | 5.35 | 0.90 | <0.001 |
| 18.0 | 53.80 | 0.96 | 25.58 | 0.98 | <0.001 |
| 24.0 | 63.14 | 0.99 | 7.62 | 0.95 | <0.001 |
| | $V_m$ Hyperpolarization (−)/Depolarization (+) Immediately after Fresh Buffer Wash | | | | |
| | | | *mV min*$^{-1}$ | | |
| 0.3 | 0.28 | 0.86 | −0.01 | 0.19 | 0.584 |
| 2.0 | 0.26 | 0.87 | −1.78 | 0.96 | 0.051 |
| 3.0 | −1.28 | 0.96 | −0.82 | 0.88 | 0.267 |
| 6.0 | −1.88 | 0.95 | −2.02 | 0.96 | 0.318 |
| 12.0 | −1.91 | 0.95 | −1.30 | 0.83 | 0.086 |
| 18.0 | −1.75 | 0.96 | −1.14 | 0.93 | 0.062 |
| 24.0 | 0.14 | 0.19 | 1.60 | 0.85 | 0.217 |

[a] *R*, Correlation coefficient. [b] *P*, significant $0.05 > P > 0.01$; highly significant <0.001.

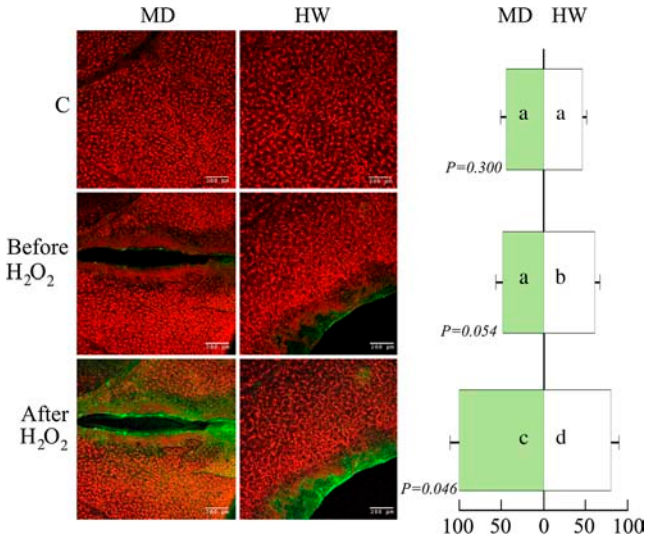


**Figure 7.** False-color image analysis reconstructions from confocal laser-scanning microscope observations and fluochemical intracellular $Ca^{2+}$ determination and image analysis in HW and MD lima bean leaves. The green fluorescence refers to binding of Fluo-3 AM with $Ca^{2+}$, whereas the chloroplasts are evidenced by a bright red color caused by chlorophyll fluorescence. As expected, HW causes a superior release of $Ca^{2+}$ than in MD. Addition of 15 mM $H_2O_2$ prompts an increased $Ca^{2+}$ release in both HW and MD tissues; however, release in MD was significantly higher. Metric bars are indicated on figures. $Ca^{2+}$ is expressed as relative percentage assuming 100% the highest value obtained. The same letter indicates nonsignificant differences.

activation of downstream responses in several plant cells (Blume et al., 2000). However, when 250 $\mu$M EGTA was applied to MD (Fig. 8A) and HW (Fig. 8B) leaves, no significant differences were found in comparison to control tissues (i.e. tissues perfused with the sole 15 mM $H_2O_2$).

Previous work demonstrated that in lima bean the use of Verapamil, a voltage-gated $Ca^{2+}$ channel antagonist, reduced the $Ca^{2+}$ influx after MD and HW (Maffei et al., 2004). Preincubation of lima bean leaves with 100 $\mu$M Verapamil was found to completely suppress $H_2O_2$-dependent $V_m$ depolarization in MD leaves (Fig. 8A). Increased values of $[Ca^{2+}]_{cyt}$ may also depend on release of $Ca^{2+}$ from internal stores. Ruthenium red has been successfully used as an inhibitor of $Ca^{2+}$ release from internal stores (Price et al., 1994). After incubation of MD and HW leaves with ruthenium red, application of 15 mM $H_2O_2$ showed the same effects. In both MD and HW leaves, ruthenium red completely suppressed $V_m$ depolarization (Fig. 8, A and B).

### ROS-Scavenging Enzyme Activities and Quantitative Reverse Transcription-PCR

To gain more insight into the sequence of the early response events of herbivore-damaged plants following $H_2O_2$ production, we analyzed the transcript accumulation and the enzymatic activities of ROS scavenging enzymes. The analysis was performed on enzyme activity and gene transcriptional levels of six selected ROS-scavenging enzymes, namely, SOD, ascorbate peroxidase (APX), peroxidase (PX), glutathione reductase (GR), GPX, and catalase (CAT), following MD or HW by larvae of *S. littoralis*. Interestingly, the transcript levels of genes coding for APX and GPX were only scarcely enhanced while the activity of both enzymes raised 6 h after both treatments (MD and HW). On the other hand, CAT activity and gene expression started to rise 1 h after herbivory; MD did not affect this enzyme at all. The other $H_2O_2$-scavenging enzymes, namely, SOD, PX, and GR, displayed increased activity 6 h after the onset of herbivore feeding. Following MD, their expression level remained low. Accordingly, most of the ROS-scavenging enzymes require an induction period of at least a few hours to become active (Fig. 10).

## DISCUSSION

$H_2O_2$ plays a dual role in plant cells; at low concentrations, it acts as a second messenger involved in

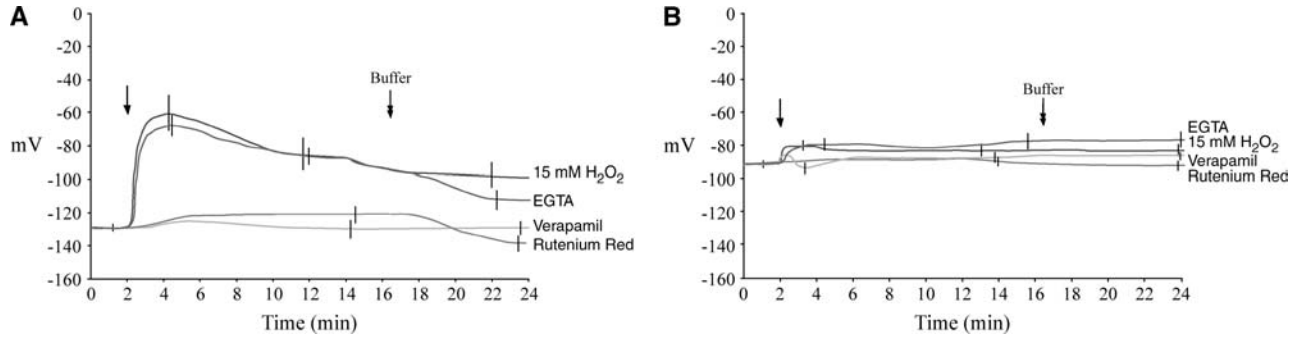


**Figure 8.** Effect of chelation of extracellular $Ca^{2+}$ by EGTA and inhibition of $Ca^{2+}$ uptake/release by specific inhibitors on $H_2O_2$-dependent $V_m$ depolarization in MD (A) and HW (B) lima bean leaves. Effect of EGTA on $H_2O_2$-dependent $V_m$ depolarization in MD (A) and HW (B) leaves is shown. Effect of $Ca^{2+}$ uptake/release inhibitors on $H_2O_2$-dependent $V_m$ depolarization in MD (A) and HW (B) leaves is shown. See text for explanation. The effect of 15 mM $H_2O_2$ without the use of inhibitors is indicated; metric bars represent SD.

signaling, and at high concentrations it is part of direct defense and may also lead to programmed cell death (Vandenabeele et al., 2003). One of the questions that remains unresolved is how $H_2O_2$ levels can trigger different responses (Kovtun et al., 2000; Neill et al., 2002); however, the ultimate question on how $H_2O_2$ is perceived and transmitted within plant cells remains unanswered, even though several candidate genes have been identified that are involved in oxidative stress sensing and signal transduction (Vandenabeele et al., 2003). In plant-pathogen interactions, plant receptor proteins perceive pathogen-derived or interaction-dependent signals, followed by downstream signaling events, including ion fluxes (Ebel and Mithöfer, 1998). Induced defense response includes the generation of ROS and NO as well as direct induction of genes, whereas amplification of the signal occurs through the generation of additional molecules (such as $Ca^{2+}$, oxylipins, or ethylene). Redox status alterations trigger mechanisms for cell protection, lipid peroxidation leads to new signaling molecules, while cross talk between the various activated signaling cascades appears to coordinate the response (Hammond-Kosack and Jones, 2000). Undoubtedly, wounding is one of the common events in plant interactions with pathogens and herbivores. Nevertheless, herbivores can cause larger and faster damage in attacked leaves where cell walls are damaged and the remaining tissues experience all the consequences of cell disruption. $H_2O_2$ is often generated or even overproduced in response to wounding in the cell walls and in the vascular bundle cells. It can be readily transported in water through the apoplast and diffuse initially into the cells adjacent to each vein (Orozco-Cárdenas et al., 2001). In MD and HW lima bean leaves, the accumulation of $H_2O_2$ at high levels in cell walls adjacent to intercellular spaces in the spongy mesophyll could be explained by the rapid evaporation of water in these air-filled spaces, together with the lower ROS-scavenging activity at these sites. This also might represent a defense strategy for the plant because wounds and the intercellular spaces are paths for subsequent secondary invasion by microbial pathogens (Bestwick et al., 1997; Orozco-Cárdenas et al., 2001). HW leaves showed higher production of $H_2O_2$ with respect to MD leaves. ROS have been associated with plant herbivore interactions, and oxidative changes in the plants correspond with oxidative damage in the midguts of insects feeding on previously wounded plants (Bi and Felton, 1995). The finding that mitochondria and/or peroxisomes are stained by Amplex Red indicates that in HW $H_2O_2$ can be produced also in the protoplast (Fig. 4). Besides, peroxisomes, which are well known to be involved in $H_2O_2$ breakdown through the action of CAT, have recently been found to be an important source of ROS (Corpas et al., 2001), while accumulation of ROS in mitochondria has been found to play a crucial role in programmed cell death (Maxwell et al., 2002; Foyer and Noctor, 2005). In response to herbivores, $H_2O_2$ levels are likely to be elevated as long as the attacks persist. In tomato plants (*Lycopersicon esculentum*) that constitutively express prosystemin, a precursor of systemin that functions in the cascades of a long-distance systemic signaling, the levels of $H_2O_2$ are constitutively elevated and may provide an early defense barrier (Orozco-Cárdenas and Ryan, 1999). Direct oxidative injury to insect midguts and damage to the nutritive and antioxidant components of the plants may be one of the ways plant counterattack herbivore feeding activity. According to Dangl et al. (1996), the presence of $H_2O_2$ in the plant in response to herbivory, before any pathogen invasion, could be advantageous because timing of the induction of defense responses can be an important factor in the success or failure of plants to defend against pathogen attacks. This is particularly true in *S. littoralis*-lima bean interaction since feeding insects introduce regurgitate from the foregut containing microorganisms into the freshly damaged leaf.

Signaling during HR does not only involve the passage of $H_2O_2$ from the apoplast, across the membrane into cytosol. This suggests that apoplast-specific components might be the source of additional signals, the generation of which requires locally high ROS levels that cannot be supplied by diffusion of intracellular $H_2O_2$ (Foyer and Noctor, 2005; Mur et al., 2005). MD lima bean leaves reacted fast and dramatically to $H_2O_2$ by inducing a strong $V_m$ depolarization. However, HW leaves already showed a reduced starting $V_m$ with the consequence of a dramatically lower or even no responsiveness to $H_2O_2$ application (Fig. 8). The depolarization of the $V_m$ by the action of HW is thus linked to a reduction of downstream responses of attacked leaves to signaling molecules such as $H_2O_2$, and the increased production of $H_2O_2$ in HW leaves indicates a possible threshold heightening of the plant $H_2O_2$-sensing system, with a consequent increased production of $H_2O_2$.

$H_2O_2$ burst often has been associated with the activation of cascade signaling events. A close interaction exists between $H_2O_2$ and cytosolic calcium in response to biotic and abiotic stimuli both in plants (Sanders et al., 1999; Murata et al., 2001; Sagi and Fluhr, 2001; Yang and Poovaiah, 2002; Foreman et al., 2003) and animals (Castro et al., 2004; Redondo et al., 2004; Rosado et al., 2004; Tabet et al., 2004) systems (see Hepler, 2005, for a historical perspective assay). The same independent assay using transgenic soybean cell suspensions that was successfully applied to analyze the activities of herbivore regurgitate components (Maffei et al., 2004) was fundamental to demonstrate that $H_2O_2$ is also able to elicit $[Ca^{2+}]_{cyt}$ release (Fig. 5). The upper level of soybean cell culture responsiveness to $H_2O_2$ corresponds to the lower level in both MD and HW lima bean leaves. This situation reflects the higher sensitivity of cell suspension cultures compared to plant tissues and should be considered for further comparisons when aequorin is used to evaluate activities of molecules involved in signaling processes. A rapid increase in $[Ca^{2+}]_{cyt}$ has also been observed at the bite

zone in lima bean (Maffei et al., 2004); however, exogenous addition of $H_2O_2$ triggered an enhanced $Ca^{2+}$ release in MD rather than in HW leaves. In animal systems, the mode of ROS generation is very sensitive to $V_m$ depolarization, and the optimal conditions for ROS generation require a hyperpolarized $V_m$ (Votyakova and Reynolds, 2001). This is in line with our hypothesis that the general $V_m$ depolarization experienced by plants attacked by herbivores is part of a strategy aimed to suppress signaling cascades in plants and

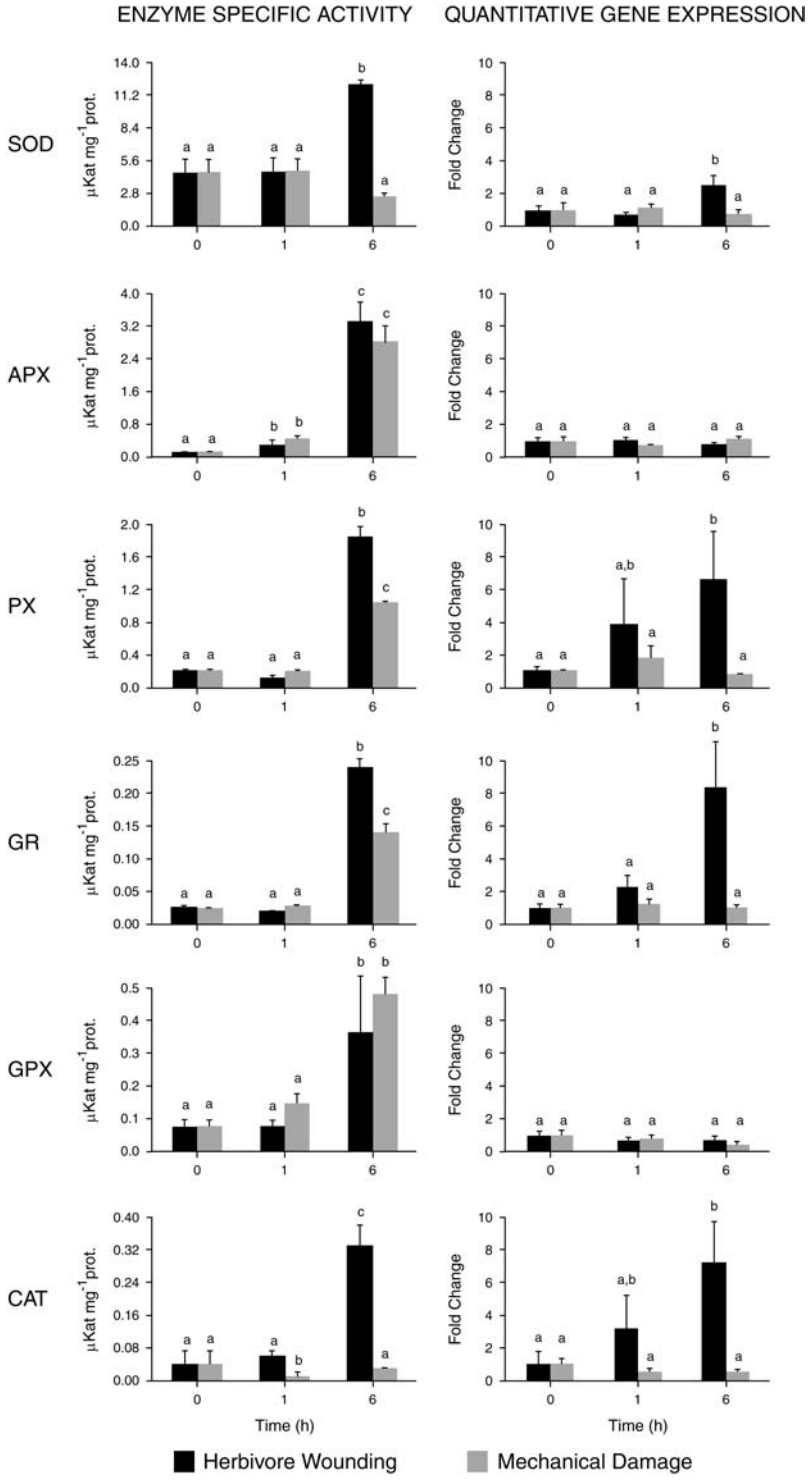


**Figure 9.** Enzyme activity and gene expression of various ROS-scavenging enzymes. Enzyme activity and quantitative gene expression was assayed at time zero (immediately after HW or MD) and after 1 and 6 h. Metric bars indicate SD. In each graph, the same letter indicates nonsignificant differences.

eventually reduce the capability to induce defenses. In this context, the parallel increase of $H_2O_2$ after HW on the one hand and the herbivore-induced $V_m$ depolarization on the other hand may represent a strategy of the plant to produce toxic $H_2O_2$ and of the herbivore to reduce $H_2O_2$ production by $V_m$ depolarization.

In plants, membrane depolarization is involved in various signal transduction pathways (Ward et al., 1995; White, 2000; Kurusu et al., 2004). Electrophysiological studies revealed the existence of plasma membrane-localized $Ca^{2+}$-permeable channels activated by membrane de- or hyperpolarization in response to external stimuli (for review, see White, 2000). These channels are postulated to play pivotal roles in early steps of a variety of signal transduction networks, such as abscisic acid-induced stomatal closure (Hamilton et al., 2000; Pei et al., 2000), defense responses (Klüsener et al., 2002), tip growth in rhizoid cells (Taylor et al., 1996), and growth of root apex (Kiegle et al., 2000). To better elucidate the role of $Ca^{2+}$ variations and the experienced $V_m$ depolarization upon $H_2O_2$ treatment, we used two $Ca^{2+}$ channel inhibitors and a $Ca^{2+}$ chelating agent. In a previous work we observed that the use of the voltage-gated $Ca^{2+}$ channel antagonist verapamil was able to reduce calcium influx in HW lima beans (Maffei et al., 2004). In MD leaves, verapamil and ruthenium red, a potent inhibitor of the release of $Ca^{2+}$ from internal stores, completely suppressed $H_2O_2$-induced $V_m$ depolarization (Fig. 8A), whereas the use of the $Ca^{2+}$ chelator EGTA did not exert any effect on both MD and HW leaves. Evidently, the removal of free $Ca^{2+}$ from the extracellular space (and buffer solution) was not sufficient to abolish $V_m$ depolarization. On the other hand, the blockage of voltage-gated channels and internal store release of $Ca^{2+}$ indicated that these two sources of $Ca^{2+}$ could be associated with $V_m$ depolarization. However, we cannot exclude that both Verapamil and ruthenium red may target the same calcium pool in this system.

High enzyme activity and/or gene expression of ROS-scavenging systems belong to the later responses following herbivore attack (Fig. 10). In fact, SOD, one

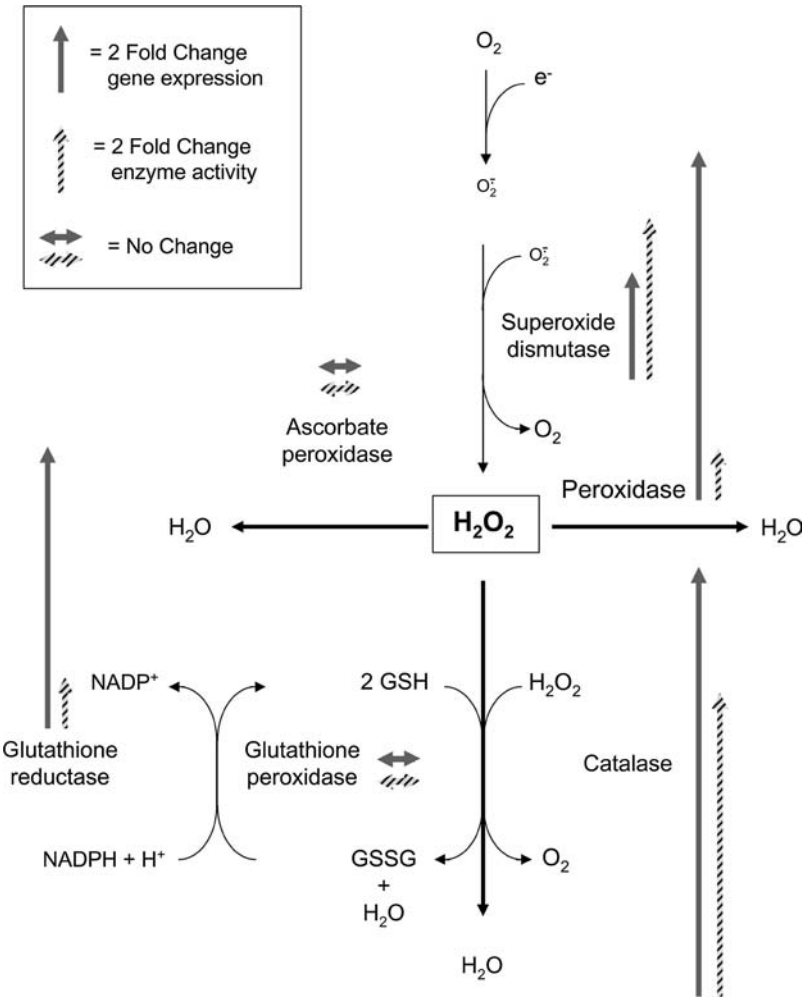


**Figure 10.** Overview on $H_2O_2$-scavenging enzymes and FCR between enzyme activity and gene expression in HW and MD lima bean leaves after 6 h. x-fold change metrics is indicated.

of the early enzymes involved in the reduction of the superoxide anion generated either by Mehler reaction and photorespiration or by the reduction of molecular oxygen in mitochondria and oxidase reaction (Ishikawa et al., 1996), is activated at the gene transcription and enzyme activity levels only after 6 h. On the other hand, the basal activity of SOD was high at zero and 1 h after treatment in both HW and MD leaves, but dropped in MD leaves after 6 h. The latter finding is consistent with the increase of $H_2O_2$ in HW leaves with time (compare Figs. 2, 3, and 9). Gene activation of CAT started earlier (after 1 h) and reached the highest activity at 6 h. This enzyme, along with PX, is directly involved in the disruption of $H_2O_2$, and their activation indicates the effort of attacked plants to reduce oxidative damage. However, a direct comparison between SOD activity and CAT-PX activities explains why $H_2O_2$ increases with time. In fact, after 6 h SOD activity is about 7- and 37-fold higher than that of the PX and CAT, respectively (Fig. 9). The highest x-fold change ratio (FCR) between HW and MD activities concerning gene up-regulation was found for CAT, which also showed the highest FCR for enzyme activity. For CAT, PX, and GR, FCR gene up-regulation was more evident than FCR enzyme activity, whereas SOD showed a superior FCR enzyme activity when compared to FCR gene up-regulation.

The low activity of APX (a typical chloroplastic enzyme; Ishikawa et al., 1996) is in agreement with the lack of Amplex Red staining observed in chloroplasts with CLSM (Fig. 4) and suggests a major role of nonphotosynthetic $H_2O_2$ production after herbivore attack. Glutathione directly reduces most active oxygen species and also scavenges $H_2O_2$ via GPX, which is involved in the detoxification of lipid peroxides rather than $H_2O_2$ per se (Noctor and Foyer, 1998; Nagalakshmi and Prasad, 2001; Chen et al., 2004; Foyer and Noctor, 2005). This might explain the almost identical GPX activity between HW and MD, even though it is generally believed that wounding caused increased GPX activity (Fig. 10).

In conclusion, these results clearly demonstrate that one of the strategies of successful herbivore attack by *S. littoralis* on lima bean is the immediate lowering of $V_m$ to a significant depolarized state, which in turn reduces the ability of the plant to react to wound-induced signals. The depolarized $V_m$ reduces the ability of the leaf to respond to at least one of the ROS, $H_2O_2$, and despite lowered $V_m$ this molecule is overproduced. An open question remains the characterization of the origin and the nature of the molecule responsible for $V_m$ depolarization after HW.

## MATERIALS AND METHODS

### Plant and Animal Material

Feeding experiments were carried out using the lima bean (*Phaseolus lunatus* cv Ferry Morse var. Jackson Wonder Bush). Individual plants were grown from seed in a plastic pot with sterilized potting soil at 23°C and 60% humidity using daylight fluorescent tubes at approximately 270 $\mu$E $m^{-2}$ $s^{-1}$ with a photophase of 16 h. Experiments were conducted with 12- to 16-d-old seedlings showing two fully developed primary leaves, which were found to be the most responsive leaves.

Larvae of *Spodoptera littoralis* (Boisd.; Lepidoptera, Noctuidae) were grown in petri dishes at long photoperiod (14–16 h photophase) and 22°C to 24°C as described (Maffei et al., 2004).

### Chemicals

$H_2O_2$ (30%), cerium chloride, $H_2$DCF-DA, Fluo-3 AM, and Verapamil were purchased from Fluka Biochemika; DAB, EGTA, and ruthenium red were from Sigma/Aldrich. Synthetic coelenterazine was from Calbiochem. Amplex Red Hydrogen Peroxide/Peroxidase Assay kit (A-22188) was purchased from Molecular Probes.

### Membrane Potentials

Membrane potentials were determined in leaf segments. The $V_m$ was determined with glass micropipettes with a tip resistance of 4 to 10 MΩ and filled with 3 M KCl. Micropipettes were used as microsalt bridges to Ag/AgCl electrodes obtained with a Narishighe PE-21 puller and inserted vertically in the tissue by means of a micromanipulator (Maffei et al., 2004). Measurements were always performed within 15 min after MD or HW. Leaves for $V_m$ measurements were sliced after MD or HW treatment and were always equilibrated for 60 to 120 min in 5 mM MES-NaOH, pH 6.0. Having assessed after several trials no significant differences between controls (undamaged leaves sliced and immediately used for $V_m$ measurement) and MD (leaves damaged and sliced after 15 min for $V_m$ measurement), all $V_m$ data are referred only to MD. Perfusion of solutions was granted by a multichannel Ismatec Reglo peristaltic pump (flow rate 1 mL $min^{-1}$). Based on topographical and temporal determination of $V_m$ performed in a previous work, the electrode was inserted between 0.5 and 1.5 mm from the wound/bite zone, where a significant $V_m$ depolarization occurs in HW (Maffei et al., 2004). $V_m$ variations were recorded both on a pen recorder and through a digital port of a PC using a data logger. Measurements were performed after perfusion with increasing concentrations of $H_2O_2$ in both MD and HW lima bean leaves. Perfusion with 15 mM $H_2O_2$ was also performed in the presence of the inhibitors of $Ca^{2+}$ uptake/release, which were applied after MD and HW.

All chemicals were dissolved in water, which was present in the control solutions, and perfused in a 50 mM MES-Na-buffered solution, pH 6.0, containing 0.5 mM calcium sulfate and 2.5 $\mu$M dichlorophenyldimethylurea (DCMU), used to poison photosynthetic electron transfer. Several trials demonstrated that DCMU has no effect on $V_m$ when used at 2.5 $\mu$M and does not alter the ROS production during the short time of $V_m$ detection. After a period of $V_m$ stabilization, saturation of the well where leaf tissues have been placed occurred in 2 min, after which perfusion was carried out for a variable time (until stabilization of the $V_m$). Washing of the well was done by perfusing with fresh buffer. Saturation with fresh buffer took 10 to 12 min, and then the solution was allowed to perfuse until $V_m$ reached a constant value.

### Cellular and Subcellular Localization of $H_2O_2$ in HW and MD Lima Bean Leaves

#### *Histochemical Localization of $H_2O_2$ Using DAB*

Cuttings of lima bean plants were placed in 15-mL Falcon tubes containing 1 mg $mL^{-1}$ DAB dissolved in HCl-acidified (pH 3.2) distilled water. Plants were then placed overnight under moderate vacuum to allow penetration of the dye. Leaves were then mechanically damaged with a cork borer or herbivore wounded with *S. littoralis*. Leaves were sampled 1, 3, 6, and 24 h after MD or HW treatment, bleached in boiling 90% ethanol for 10 min, and mounted on glass slides. To improve staining visibility, samples were observed with the epifluorescence Nikon Eclipse E400 microscope equipped with a 450-nm filter, and pictures are presented as black and white inversed images.

#### *Subcellular Localization of $H_2O_2$ Using $CeCl_3$*

Following MD or HW treatment, small lima bean tissue pieces were excised from leaves and vacuum infiltrated with freshly prepared 5 mM $CeCl_3$ in 50 mM MOPS at pH 7.2 for 1 h. After fixation in 1.25% (v/v) glutaraldehyde

and 1.25% (v/v) paraformaldehyde in 50 mM sodium cacodylate buffer, pH 7.2, for 2 h under vacuum at room temperature, samples were kept overnight at 4°C. Subsequently, tissues were washed twice, under vacuum, for 10 min in cacodylate buffer, postfixed for 1 h in osmium tetroxide 1% (v/v) in cacodylate buffer, and washed twice in cacodylate buffer for 10 min. Tissues were then dehydrated in a graded acetone series, incubated in rising concentration of acetone-resin mixture, and then embedded and polymerized for 24 h at 60°C in Epon/Araldite resin. Thin sections were then cut with a Reichert Ultracut ultramicrotome. Staining was not performed in order not to overlay $CeCl_3$ precipitation, and thin sections mounted on 400 mesh grids were observed under the Philips CM10 transmission electron microscope.

### *CLSM Subcellular Localization of $H_2O_2$ and Active PXs Using Amplex Red*

Lima bean leaves from rooted plants in pots were herbivore wounded and mechanically damaged after incubation with the dye Amplex Red. The Molecular Probes Amplex Red Hydrogen Peroxide/Peroxidase Assay kit (A-22188) was used and dissolved in MES-Na buffer 50 mM, pH 6.0, containing 0.5 mM calcium sulfate and 5 $\mu$M DCMU, to obtain a 50 $\mu$M solution. Leaves where then mounted on a Leica TCS SP2 multiband confocal laser-scanning microscope stative without separating the leaf from the plant. Scannings were recorded from time 0 up to 180 min using the HCX PL APO 63 × /1.20 W Corr/0.17CS objective. The microscope was operated with a Laser Ar (458 nm/5 mW; 476 nm/5 mW; 488 nm/20 mW; 514 nm/20 mW), a Laser HeNe 543 nm/1.2 mW, and a Laser HeNe 633 nm/10 mW.

### *Fluorimetric Determination of $H_2O_2$ Using $H_2$DCF-DA*

Lima bean leaves from rooted plants in pots were herbivore wounded and mechanically damaged after incubation with the dye $H_2$DCF-DA. This nonfluorescent dye can cross the plasma membrane freely, and is then cleaved to its impermeable counterpart, dichlorofluorescin ($H_2$DCF), by endogenous esterases. $H_2$DCF, which accumulates in the cell, functions as a reporter of cytoplasmic $H_2O_2$ by converting upon oxidation to its fluorescent form, DCF (green fluorescence; Lee et al., 1999). $H_2$DCF-DA was dissolved in MES-Na buffer 50 mM, pH 6.0, containing 0.5 mM $CaSO_4$ and 5 $\mu$M DCMU, to obtain a 50-$\mu$M solution. Leaves were then mounted on an Olympus FLUOview confocal laser-scanning microscope stative without separating the leaf from the plant. Scannings were recorded from time 0 up to 180 min. The microscope is operated with a Krypton/Argon laser at 488 nm and 568 nm wavelengths: the first wavelength excitates the dye, resulting in emission of green light, and the second mostly excitates chloroplasts, which emit red fluorescence. Images generated by the FluoView software were analyzed using the public domain NIH Image J program (developed at the United States National Institutes of Health and available on the Internet at http://rsb.info.nih.gov/nih-image).

### Intracellular Calcium Variation Determination

Fluo-3 AM (more permeant for cells), purchased as a stock solution in dimethyl sulfoxide, was diluted in 50 mM MES-Na buffer, pH 6.0, by addition of 0.5 mM $CaSO_4$, 2.5 $\mu$M DCMU to reach the concentration of 5 $\mu$M. This resulting solution was used for an initial treatment of lima bean leaves not separated from the plant: The leaf was gently fixed over a glass slide, and a drop (about 20 $\mu$L) of 5 $\mu$M Fluo-3 AM solution was applied and covered with another glass slide. Thirty minutes after treatment with Fluo-3 AM, the leaf was mounted on an Olympus FLUOview confocal laser-scanning microscope stative without separating the leaf from the plant. After 30 min, 15 mM $H_2O_2$ were added to MD and HW, and Fluo-3 AM fluorescence was recorded. Measurements were taken in intact leaves, with leaves wounded mechanically and after herbivore feeding, both in the presence and absence of exogenous calcium. The Olympus confocal laser-scanning microscope is operated as above. Images generated by the FluoView software were analyzed using the public domain NIH Image J program (developed at the United States National Institutes of Health and available on the Internet at http://rsb.info.nih.gov/nih-image).

### Aequorin-Dependent Luminescence Measurements

Transgenic soybean (*Glycine max*) 6.6.12 cell lines carrying the stably integrated plasmid *pGNAequ/neo2* and expressing apoaequorin (Mithöfer et al., 1999) were used to reconstitute aequorin in vivo with 10 $\mu$M synthetic coelenterazine on a shaker (125 rpm) in the dark for 24 h. The $Ca^{2+}$-specific luminescence (470 nm) was measured in a final volume of 200 $\mu$L using a digital luminometer (Bio-Orbit 1250) as described (Mithöfer et al., 1999; Mithöfer and Mazars, 2002). Treatments with various compounds were performed by adding 1 to 10 $\mu$L of different concentrations of aqueous stock solutions to the cell suspension culture. Mixing time for the addition of any compound was 5 to 7 s. In each experiment, the concentration of reconstituted aequorin was not limiting under any of the experimental conditions, with a maximal consumption not exceeding 10%. The residual aequorin was completely discharged by adding 200 $\mu$L of 20% ethanol containing 2 M $CaCl_2$ (final concentration 10% and 1 M, respectively). The resulting luminescence was used to estimate the total amount of aequorin present in various experiments to determine the rate of aequorin consumption for the calculation of the cytosolic $Ca^{2+}$ concentrations according to Allen et al. (1977).

### ROS-Scavenging Enzyme Activity

Leaves were collected immediately after and at 1 h and 6 h after HW or MD. Intact leaves pooled from five plants were frozen in liquid $N_2$ and stored at −80°C before enzyme extraction. ROS scavenger enzymes were extracted following the method of Zhang and Kirkham (1996) with some modifications. All operations were carried out at 4°C. Plant material was ground with mortar and pestle under liquid nitrogen in cold 50 mM sodium phosphate, pH 7.5, containing 250 mM Suc, 1.0 mM EDTA, 10 mM KCl, 1 mM $MgCl_2$, 0.5 mM phenylmethylsulfonyl fluoride, 0.1 mM dithiothreitol, and 1% (w/v) polyvinylpolypyrrolidone in a 6:1 proportion (w/v). The homogenate was then filtered through eight layers of cheesecloth and centrifuged at 25,000*g* for 20 min at 4°C. The supernatant was brought to 80% saturation with addition of solid ammonium sulfate $(NH_4)_2SO_4$ and allowed to stir gently for several hours at 4°C. After centrifugation at 28,000*g* for 45 min at 4°C, pellets, containing most of enzyme activity, were resuspended in a small volume of 50 mM sodium phosphate, pH 7.5, and used directly for enzyme assays.

### *SOD (EC 1.15.1.1)*

The activity of SOD was measured according to Krishnan et al. (2002). This method tests the ability of SOD to inhibit the reduction of nitro blue tetrazolium by the superoxide anion generated photochemically. One milliliter of assay mixture consisted of 50 mM Na-P buffer, pH 7.8, 13 mM Met, 75 $\mu$M nitro blue tetrazolium, 2 $\mu$M riboflavin, 0.1 mM EDTA, and enzyme extract. Riboflavin was added last, the samples were placed 30 cm below a light source (4,000 lux), and the reaction was allowed to run for 15 min. The reaction was stopped by switching off the light. A nonirradiated reaction mixture, which was run in parallel, did not develop color and served as a control. The absorbance was read at 560 nm.

### *APX (EC 1.11.1.11)*

APX activity was determined from the decrease in $A_{290}$, due to the $H_2O_2$-dependent oxidation of ascorbate ($\varepsilon$ = 2.8 $mM^{-1}$ $cm^{-1}$; Zhang and Kirkham, 1996). The 1-mL reaction mixture contained 50 mM Na-P, pH 7.0, 0.5 mM ascorbic acid, 0.1 mM $H_2O_2$, 0.1 mM EDTA, and enzyme.

### *PX (EC 1.11.1.7)*

PX activities were measured as oxidation of guaiacol ($\varepsilon$ = 26.6 $mM^{-1}$ $cm^{-1}$) in the presence of $H_2O_2$ (Zhang and Kirkham, 1996). The reaction mixture contained 50 mM Na-P, pH 7.0, 0.33 mM guaiacol, 0.27 mM $H_2O_2$, and enzyme extract in 1.0 mL final volume. The reaction was started by addition of guaiacol and followed spectrophotometrically at 470 nm.

### *GR (EC 1.8.1.10)*

GR activity was determined at 340 nm by following the oxidation of NADPH ($\varepsilon$ = 6.2 $mM^{-1}$ $cm^{-1}$) at 340 nm (Zhang and Kirkham, 1996). The reaction mixture contained 100 mM Na-P, pH 7.5, 0.2 mM NADPH, 0.5 mM glutathione disulfide, and enzyme extract in a 1.0 mL final volume at 30°C. The reaction was started by adding glutathione disulfide.

### *GPX (EC 1.11.1.9)*

GPX was assayed indirectly, as described by Anderson and Davis (2004). The reaction contained 125 mM K-P buffer, pH 7.0, 1.2 mM cumene hydroperoxide, 1.25 mM EDTA, 1.25 mM sodium azide, 1.0 mM glutathione, 0.25 mM NADPH, 0.6 IU of yeast GR (Sigma Type III), and enzyme extract in a final volume of 1 mL. After incubation for 10 min at 25°C with all the reagents except cumene hydroperoxide, the reaction was started with cumene hydroperoxide. Decrease of NADPH at 340 nm was corrected for nonenzymatic controls.

### *CAT (EC 1.11.1.6)*

CAT activities were assayed spectrophotometrically by monitoring the change in $A_{240}$ due to the decreased absorption of $H_2O_2$ ($\varepsilon$ $H_2O_2$ = 39.4 $mM^{-1}$ $cm^{-1}$; Zhang and Kirkham, 1996). The reaction mixture in 1 mL final volume contained 50 mM Na-P, pH 7.0, 15 mM $H_2O_2$, and enzyme extract. The reaction was initiated by addition of $H_2O_2$.

## Soluble Protein Determination

Soluble protein concentration was evaluated by the method of Bradford (1976) using bovine serum albumin as a standard.

## Real-Time PCR

Total RNA was isolated from leaf tissues of MD and HW plants at the time zero, and after 1 and 6 h following MD or HW using the Concert Plant RNA Reagent (Invitrogen) following the manufacturer's protocol. The total RNA was purified to eliminate genomic DNA using Qiagen RNeasy Plant RNA kit and RNase-Free DNase set (Qiagen). First-strand cDNA was synthesized using SuperScript III Reverse Transcriptase (Invitrogen), oligo$(dT)_{12\text{-}18}$ primer, and 1 $\mu$g of total RNA at 50°C for 50 min. Primers for real-time PCR were designed using the Primer 3 software (http://frodo.wi.mit.edu/cgi-bin/primer3/primer3_www.cgi) for a length of the resulting PCR product of approximately 200 bp (see below). The real-time PCR was done on an Mx3000P Real-Time PCR system (Stratagene). The process was performed with 25 $\mu$L of reaction mixture consisting of 12.5 $\mu$L of 2× Brilliant SYBR Green QPCR Master Mix (Stratagene), cDNA (1 $\mu$L from 20 $\mu$L of each reverse transcription [RT] product pool), 100 nM primers, and 30 mM ROX as a reference dye. The following protocol was applied: initial polymerase activation of 10 min at 95°C; and 40 cycles of 30 s at 95°C, 60 s at 55°C, and 30 s at 72°C. PCR conditions were determined by comparing threshold values in dilution series of the RT product, followed by non-RT template control and nontemplate control for each primer pair. Relative RNA levels were calibrated and normalized with the level of actin mRNA (GenBank accession no. DQ159907).

Primers used for real-time PCR were as follows: *ACT1*, accession number DQ159907, forward primer 5′-AGGCTCCTCTTAACCCCAAG-3′, reverse primer 5′-GTGGGAGAGCATAACCCTCA-3′; *AP1*, accession number DQ004738, forward primer 5′-AGGAGCGTTCTGGATTTGAG-3′, reverse primer 5′-AATCAGCGAAGAACGCATCT-3′; *CAT1*, accession number DQ004737, forward primer 5′-GCCGCATGGTCTTGAATAAG-3′, reverse primer 5′-ATTTGGGTGCATTAGCAGGA-3′; *GP1*, accession number DQ004739, forward primer 5′-AACAGGAAACTCAGCCTTGAA-3′, reverse primer 5′-ATTGTCAACGTTGCCTCACA-3′; *GR1*, accession number DQ159906, forward primer 5′-GCCCCTTCATTCCTGATATTC-3′, reverse primer 5′-TCGTCAAATCCCCTCAGAAC-3′; *PER1*, accession number DQ159909, forward primer 5′-GACCCTGTCATGGACCAAAC-3′, reverse primer 5′-CAATGCCCTTGGTCCTCTTA-3′; and *SOD1*, accession number DQ159910, forward primer 5′-AAGCACCACAGGGCTTATGT-3′, reverse primer 5′-ATGGTTTTCCACCTCCACCT-3′.

## Statistics

At least five repetitions were used for the statistical treatment of the data. More than five repetitions contributed to the mean values given in Figures 6 and 8. The data are expressed as mean values; metric bars indicate the SD. To evaluate the difference significance of the control and the treatments at the given concentrations, ANOVA was performed. Tamhane's T2 test was used to determine post-hoc differences.

## ACKNOWLEDGMENTS

We are indebted to Dr. G. Trautmann (Bayer AG) for supplying us with egg clutches of lepidopteran larvae and A. Berg for caterpillar rearing. We also thank H. Maischak for help with statistical analysis.

Received September 29, 2005; revised January 12, 2006; accepted January 12, 2006; published January 27, 2006.

## LITERATURE CITED

**Allen D, Blinks JR, Prendergast FG** (1977) Aequorin luminescence: relation of light emission to calcium concentration—a calcium-independent component. Science **195:** 996–998

**Anderson J, Davis DG** (2004) Abiotic stress alters transcript profiles and activity of glutathione-*S*-transferase, glutathione peroxidase and glutathione reductase in *Euphorbia esula*. Physiol Plant **120:** 421–433

**Angelini R, Manes F, Federico R** (1990) Spatial and functional correlation between diamine-oxidase and peroxidase activities and their dependence upon de-etiolation and wounding in chick-pea stems. Planta **182:** 89–96

**Bergey DR, Orozco-Cárdenas ML, de Moura DS, Ryan CA** (1999) A wound- and systemic-inducible polygalacturonase in tomato leaves. Proc Natl Acad Sci USA **96:** 1756–1760

**Bestwick CS, Brown IR, Bennett MHR, Mansfield JW** (1997) Localization of hydrogen peroxide accumulation during the hypersensitive reaction of lettuce cells to *Pseudomonas syringae* pv *phaseolicola*. Plant Cell **9:** 209–221

**Bestwick CS, Brown IR, Mansfield JW** (1998) Localized changes in peroxidase activity accompany hydrogen peroxide generation during the development of a nonhost hypersensitive reaction in lettuce. Plant Physiol **118:** 1067–1078

**Bi JL, Felton GW** (1995) Foliar oxidative stress and insect herbivory: primary compounds, secondary metabolites, and reactive oxygen species as components of induced resistance. J Chem Ecol **21:** 1511–1530

**Blume B, Nürnberger T, Nass N, Scheel D** (2000) Receptor-mediated increase in cytoplasmic free calcium required for activation of pathogen defense in parsley. Plant Cell **12:** 1425–1440

**Bolwell DJ** (1999) Role of active oxygen species and NO in plant defence responses. Curr Opin Plant Biol **2:** 287–294

**Bolwell GP, Wojtaszek P** (1997) Mechanisms for the generation of reactive oxygen species in plant defence: a broad perspective. Physiol Mol Plant Pathol **51:** 347–366

**Bradford MM** (1976) A rapid and sensitive method for the quantitation of microgram quantities of protein utilizing the principle of protein-dye binding. Anal Biochem **72:** 248–254

**Bradley DJ, Kjellbom P, Lamb CJ** (1992) Elicitor- and wound-induced oxidative cross-linking of a proline-rich plant cell wall protein: a novel, rapid defense response. Cell **70:** 21–30

**Castro J, Bittner CX, Humeres A, Montecinos VP, Vera JC, Barros LF** (2004) A cytosolic source of calcium unveiled by hydrogen peroxide with relevance for epithelial cell death. Cell Death Differ **11:** 468–478

**Cazalé A-C, Rouet-Mayer M-A, Barbier-Brygoo H, Mathieu Y, Laurière C** (1998) Oxidative burst and hypoosmotic stress in tobacco cell suspensions. Plant Physiol **116:** 659–669

**Chen K-M, Gong H-J, Chen G-C, Wang S-M, Zhang C-L** (2004) Gradual drought under field conditions influences the glutathione metabolism, redox balance and energy supply in spring wheat. J Plant Growth Regul **23:** 20–28

**Chen Z, Silva H, Klessig DF** (1993) Active oxygen species in the induction of plant systemic acquired resistance by salicylic acid. Science **262:** 1883–1886

**Corpas FJ, Barros JB, del Rio LA** (2001) Peroxisomes as a source of reactive oxygen species and nitric oxide signal molecules in plants. Trends Plant Sci **6:** 145–150

**Dangl JL, Dietrich RA, Richberg MH** (1996) Death don't have no mercy: cell death programs in plant-microbe interactions. Plant Cell **8:** 1793–1807

**Devlin WS, Gustine DL** (1992) Involvement of the oxidative burst in phytoalexin accumulation and the hypersensitive reaction. Plant Physiol **100:** 1189–1195

**Ebel J, Mithöfer A** (1998) Early events in the elicitation of plant defence. Planta **206:** 335–348

**Felton G, Summers CB, Mueller AJ** (1994) Oxidative responses in soybean foliage to herbivory by bean leaf beetle and three-cornered alfalfa hopper. J Chem Ecol **20:** 639–649

**Foreman J, Demidchik V, Bothwell JHF, Mylona P, Miedema H, Torres MA, Linstead P, Costa S, Brownlee C, Jones JDG, et al** (2003) Reactive oxygen species produced by NADPH oxidase regulate plant cell growth. Nature **422:** 442–446

**Foyer CH, Lopez Delgado H, Dat JF, Scott IM** (1997) Hydrogen peroxide and glutathione-associated mechanisms of acclimatory stress tolerance and signalling. Physiol Plant **100:** 241–254

**Foyer CH, Noctor G** (2005) Redox homeostasis and antioxidant signaling: a metabolic interface between stress perception and physiological responses. Plant Cell **17:** 1866–1875

**Gus-Mayer S, Naton B, Hahlbrock K, Schmelzer E** (1998) Local mechanical stimulation induces components of the pathogen defense response in parsley. Proc Natl Acad Sci USA **95:** 8398–8403

**Hamilton DWA, Hills A, Kohler B, Blatt MR** (2000) $Ca^{2+}$ channels at the plasma membrane of stomatal guard cells are activated by hyperpolarization and abscisic acid. Proc Natl Acad Sci USA **97:** 4967–4972

**Hammond-Kosack K, Jones JDG** (2000) Responses to plant pathogens. *In* B Buchanan, W Gruissem, R Jones, eds, Biochemistry and Molecular Biology of Plants. American Society of Plant Physiologists, Rockville, MD, pp 1102–1156

**Hepler PK** (2005) Calcium: a central regulator of plant growth and development. Plant Cell **17:** 2142–2155

**Hiraga S, Ito H, Yamakawa H, Ohtsubo N, Seo S, Mitsuhara I, Matsui H, Honma M, Ohashi Y** (2000) A HR-induced tobacco peroxidase gene is responsive to spermine, but not to salicylate, methyl jasmonate, and ethephon. Mol Plant Microbe Interact **13:** 210–216

**Ishikawa T, Takeda T, Kohno H, Shigeoka S** (1996) Molecular characterization of *Euglena* ascorbate preoxidase using monoclonal antibody. Biochim Biophys Acta **1290:** 69–75

**Jacks TJ, Davidonis GH** (1996) Superoxide, hydrogen peroxide, and the respiratory burst of fungally infected plant cells. Mol Cell Biochem **158:** 77–79

**Kiegle E, Gilliham M, Haseloff J, Tester M** (2000) Hyperpolarization activated calcium currents found only in cells from the elongation zone of *Arabidopsis thaliana* roots. Plant J **21:** 225–229

**Klüsener B, Young JJ, Murata Y, Allen GJ, Mori IC, Hugouvieux V, Schroeder JI** (2002) Convergence of calcium signaling pathways of pathogenic elicitors and abscisic acid in Arabidopsis guard cells. Plant Physiol **130:** 2152–2163

**Kovtun Y, Chiu WL, Tena G, Sheen J** (2000) Functional analysis of oxidative stress-activated mitogen-activated protein kinase cascade in plants. Proc Natl Acad Sci USA **97:** 2940–2945

**Krishnan N, Chattopadhyay S, Kundu JK, Chaudhuri A** (2002) Superoxide dismutase activity in haemocytes and haemolymph of *Bombix mori* following bacterial infection. Curr Sci **83:** 321–325

**Kurusu T, Sakurai Y, Miyao A, Hirochika H, Kuchitsu K** (2004) Identification of a putative voltage-gated $Ca^{2+}$-permeable channel (OsTPC1) involved in $Ca^{2+}$ influx and regulation of growth and development in rice. Plant Cell Physiol **45:** 693–702

**Lamb C, Dixon RA** (1997) The oxidative burst in plant disease resistance. Annu Rev Plant Physiol Plant Mol Biol **48:** 251–275

**Lee S, Choi H, Suh S, Doo I-S, Oh K-Y, Choi EJ, Schroeder Taylor AT, Low PS, Lee Y** (1999) Oligogalacturonic acid and chitosan reduce stomatal aperture by inducing the evolution of reactive oxygen species from guard cells of tomato and *Commelina communis*. Plant Physiol **121:** 147–152

**Legendre L, Rueter S, Heinstein PF, Low PS** (1993) Characterization of the oligogalacturonide-induced oxidative burst in cultured soybean (*Glycine max*) cells. Plant Physiol **102:** 233–240

**Leitner M, Boland W, Mithöfer A** (2005) Direct and indirect defences induced by piercing-sucking and chewing herbivores in *Medicago truncatula*. New Phytol **167:** 597–606

**Levine A, Tenhaken R, Dixon R, Lamb C** (1994) $H_2O_2$ from the oxidative burst orchestrates the plant hypersensitive disease resistance response. Cell **79:** 583–593

**Low PS, Merida JR** (1996) The oxidative burst in plant defense: function and signal transduction. Physiol Plant **96:** 533–542

**Maffei M, Bossi S, Spiteller D, Mithöfer A, Boland W** (2004) Effects of feeding *Spodoptera littoralis* on lima beans leaves. I. Membrane potentials, intracellular calcium variations, oral secretions, and regurgitate components. Plant Physiol **134:** 1752–1762

**Maxwell DP, Nickels R, McIntosh L** (2002) Evidence of mitochondrial involvement in the transduction of signals required for the induction of genes associated with pathogen attack and senescence. Plant J **29:** 269–279

**Mehdy MC, Sharma YK, Sathasivan K, Bays NW** (1996) The role of activated oxygen species in plant disease resistance. Physiol Plant **98:** 365–374

**Mithöfer A, Daxberger A, Fromhold-Treu D, Ebel J** (1997) Involvement of an NAD(P)H oxidase in the elicitor-inducible oxidative burst in soybean. Phytochemistry **45:** 1101–1107

**Mithöfer A, Ebel J, Bhagwat AA, Boller T, Neuhaus-Url G** (1999) Transgenic aequorin monitors cytosolic calcium transients in soybean cells challenged with $\beta$-glucan or chitin elicitors. Planta **207:** 566–574

**Mithöfer A, Mazars C** (2002) Aequorin-based measurements of intracellular $Ca^{2+}$-signatures in plant cells. Biol Proced Online **4:** 105–118

**Mithöfer A, Schulze B, Boland W** (2004) Biotic and heavy metal stress response in plants: evidence for common signals. FEBS Lett **566:** 1–5

**Mithöfer A, Wanner G, Boland W** (2005) Effects of feeding *Spodoptera littoralis* on lima bean leaves. II. Continuous mechanical wounding resembling insect feeding is sufficient to elicit herbivory-related volatile emission. Plant Physiol **137:** 1160–1168

**Mur L, Kenton P, Draper J** (2005) *In planta* measurements of oxidative bursts elicited by avirulent and virulent bacterial pathogens suggests that $H_2O_2$ is insufficient to elicit cell death in tobacco. Plant Cell Environ **28:** 548–561

**Mur LAJ, Brown IR, Darby RM, Bestwick CS, Bi YM, Mansfield JW, Draper J** (2000) A loss of resistance to avirulent bacterial pathogens in tobacco is associated with the attenuation of a salicylic acid-potentiated oxidative burst. Plant J **23:** 609–621

**Murata Y, Pei Z-M, Mori IC, Schroeder J** (2001) Abscisic acid activation of plasma membrane $Ca^{2+}$ channels in guard cells requires cytosolic NAD(P)H and is differentially disrupted upstream and downstream of reactive oxygen species production in *abi1-1* and *abi2-1* protein phosphatase 2C mutants. Plant Cell **13:** 2513–2523

**Nagalakshmi N, Prasad MNV** (2001) Responses of glutathione cycle enzymes and glutathione metabolism to copper stress in *Scenedesmus bijugatus*. Plant Sci **160:** 291–299

**Neill S, Desikan R, Hancock J** (2002) Hydrogen peroxide signaling. Curr Opin Plant Biol **5:** 388–395

**Noctor G, Foyer CH** (1998) Ascorbate and glutathione: keeping active oxygen under control. Annu Rev Plant Physiol Plant Mol Biol **49:** 249–279

**Olson PD, Varner JE** (1993) Hydrogen peroxide and lignification. Plant J **4:** 887–892

**Orozco-Cárdenas M, Narváez-Vásquez J, Ryan CA** (2001) Hydrogen peroxide acts as a second messenger for the induction of defense genes in tomato plants in response to wounding, systemin, and methyl jasmonate. Plant Cell **13:** 179–181

**Orozco-Cárdenas ML, Ryan C** (1999) Hydrogen peroxide is generated systemically in plant leaves by wounding and systemin via the octadecanoid pathway. Proc Natl Acad Sci USA **96:** 6553–6557

**Overmyer K, Brosché M, Kangasjärvi J** (2003) Reactive oxygen species and hormonal control of cell death. Trends Plant Sci **8:** 335–342

**Pei Z-M, Murata Y, Benning G, Thomine S, Klusener B, Allen GJ, Grill E, Schroeder JI** (2000) Calcium channels activated by hydrogen peroxide mediate abscisic acid signalling in guard cells. Nature **406:** 731–734

**Price AH, Taylor A, Ripley SJ, Griffiths A, Trewavas AJ, Knight MR** (1994) Oxidative signals in tobacco increase cytosolic calcium. Plant Cell **6:** 1301–1310

**Redondo PC, Salido GM, Pariente JA, Rosado JA** (2004) Dual effect of hydrogen peroxide on store-mediated calcium entry in human platelets. Biochem Pharmacol **67:** 1065–1076

**Rosado JA, Ridondo PC, Salido GM, Gomez-Arteta E, Sage SO, Pariente JA** (2004) Hydrogen peroxide generation induces pp60(src) activation in human platelets: evidence for the involvement of this pathway in store-mediated calcium entry. J Biol Chem **279:** 1665–1675

**Sagi M, Fluhr R** (2001) Superoxide production by plant homologues of the $gp91^{phox}$ NADPH oxidase: modulation of activity by calcium and by tobacco mosaic virus infection. Plant Physiol **126:** 1281–1290

**Sanders D, Brownlee C, Harper JF** (1999) Communicating with calcium. Plant Cell **11:** 691–706

**Sanders D, Pelloux J, Brownlee C, Harper JF** (2002) Calcium and the crossroads of signalling. Plant Cell (Suppl) **14:** S401–S417

**Stennis MJ, Chandra S, Ryan CA, Low PS** (1998) Systemin potentiates the oxidative burst in cultured tomato cells. Plant Physiol **117:** 1031–1036

**Tabet F, Savoia C, Schiffrin EL, Touyz RM** (2004) Differential calcium regulation by hydrogen peroxide and superoxide in vascular smooth muscle cells from spontaneously hypersensitive rats. J Cardiovasc Pharmacol **44:** 200–208

**Taylor AR, Manison NF, Fernandez C, Wood J, Brownlee C** (1996) Spatial organization of calcium signaling involved in cell volume control in the Fucus rhizoids. Plant Cell **8:** 2015–2031

**Thordal-Christensen H, Zhang ZG, Wei YD, Collinge DB** (1997) Subcellular localization of $H_2O_2$ in plants: $H_2O_2$ accumulation in papillae and hypersensitive response during the barley-powdery mildew interaction. Plant J **11:** 1187–1194

**Vandenabeele S, Van Der Kelen K, Dat J, Gadjev I, Boonefaes T, Morsa S, Rottiers P, Slooten L, Van Montagu M, Zabeau M, et al** (2003) A comprehensive analysis of hydrogen peroxide-induced gene expression in tobacco. Proc Natl Acad Sci USA **23:** 16113–16118

**Votyakova TV, Reynolds IJ** (2001) $\Delta\Psi_m$-dependent and -independent production of reactive oxygen species by rat brain mitochondria. J Neurochem **79:** 266–277

**Ward JM, Pei ZM, Schroeder JI** (1995) Roles of ion channels in initiation of signal transduction in higher plants. Plant Cell **7:** 833–844

**White PJ** (2000) Calcium channels in higher plants. Biochim Biophys Acta **1465:** 171–189

**Yahraus T, Chandra S, Legendre L, Low PS** (1995) Evidence for mechanically induced oxidative burst. Plant Physiol **109:** 1259–1266

**Yang T, Poovaiah BW** (2002) Hydrogen peroxide homeostasis: activation of plant catalase by calcium/calmodulin. Proc Natl Acad Sci USA **99:** 4097–4102

**Zhang J, Kirkham MB** (1996) Antioxidant responses to drought in sunflower and sorghum seedlings. New Phytol **132:** 361–373